Atmospheric icing and meteorological variables
–
Full scale experiment and testing of models

Thesis for the Dr. Scient. degree

Magne A. Drage

February, 2005

The University Centre
in Svalbard
Longyearbyen, Norway

Department of Geophysics
University of Bergen
Bergen, Norway

Geophysical Institute
University of Bergen
Allegt. 70
5007 Bergen

ISBN 82-8116-006-3
ISSN 1502-5519

Reports in Meteorlogy and Oceanography
Nr. 4-2005

Preface

This thesis is a part of the Dr. scient degree submitted to the University of Bergen, Norway. The study has been funded by Forsvarsbygg, Norkring, Statnett and Telenor. Thanks to all persons involved for having the faith in the project in the starting phase. Particularly, I am grateful to Arnfinn Jenssen, who initiated the study.

For the last three and a half years I have been employed as a research fellow by the University centre in Svalbard (UNIS). The first year I had my daily work at the Norwegian Meteorological Institute at the Research and Development department, while I have been situated at the University of Bergen the last two and a half year. In this period, I have also been visiting UNIS several times, recently with a one month stay in January 2005. I am thankful to all of them for providing fine working conditions during this study.

Support from the operating personal at the field sites has been a key factor for the success of this work. I would therefore like to bring a special thanks to Odd Rutledal and Øistein Saugerud, for their excellent support during the field work. I would also like to thank Rune Stenseth for his support in the initial stage of this study.

I will also thank the co-authors of the presented papers for a close co-operation.

Thanks to Professor Yngvar Gjessing who has been my main supervisor and had the faith in my abilities in the starting phase. Thank you for all inspiration to me all the way back from my undergraduate period at UNIS.

Thanks to Amanuensis Jan Asle Olseth who has been co-supervisor, for quick response of my question, and encouragement during the study.

Last but not least my wife Sigrid deserves thanks for listening to my concerns during the work process and for putting up with my late nights of work or even absence for periods of the study.

February 2005

Magne A. Drage

1. Introduction

Atmospheric icing on structures is often a serious problem in regions with cold climate. Large economic costs, as well as human inconvenience, are the result of failures and damage. During the period 1967-1991, a large number of structures in Europe, the U.S.A., Canada and Japan have collapsed or been partly damaged due to atmospheric icing (table 1.1). In the U.S.A. alone, there have been about 140 icing-related tower failures over the last 40 years. (Mulherin, 1998). Location of structures in elevated areas represents a potential risk for problems related to icing. In order to obtain the best possible coverage, Radio - and Telecommunication require high antennas, which often need to be located in mountainous locations. The potential risk of problems related to atmospheric icing is often underestimated during the planning and building stages in such areas. Thus, ice data are rarely collected before the structure is built. This illustrates the importance of forecasting atmospheric icing, as well as determining design loads. The research history of the topic *ice and snow accretion on structures* has been reviewed by Poots (2000).

1.1 Objectives

The objective of this study has been to obtain a better understanding of the physical processes for atmospheric icing in the boundary layer of mountainous regions. By use of collected experimental data, the intention has been to test and develop existing methods for prediction of occurrence, duration and intensity of icing. The advantages and limitations of these methods have also been studied. A comparison of detailed measurements of air temperature and humidity versus height, in relation to icing measurements, is, in most cases, lacking in literature about icing.

Table 1.1. Partly damaged or collapsed structures due to icing
(Adapted from Mulherin 1988).

Year and date for failure. (Age of mast)	Mast.	Height of mast [m]	Altitude above sea level [m]	Probable load situation causing the failure.
1967 Dec. 12 (--)	Canada, Quebec, Trois Rivieres	330	--	Overload of ice and wind during an icing storm.
1969 Nov. 23 (1)	Finland, Ylläs	212	697	Overload of heavy ice acting together with light wind.
1973 Dec. 4 (0)	USA, Iowa, Alleman	610	296	Ice and wind. Top of the mast broken during construction.
1975 Jan. 11 (6)	USA, S. Dakota, Rowena	605	445	Overload of ice and strong wind during an icing storm.
1975 Mar. 27 (6)	USA, S. Dakota, Salem	477	469	Overload (galloping?) of ice and wind during an icing storm.
1978 Feb. 6 (12)	USA, Nebraska, Angora	457	1295	Fatigue due to wind induced vibrations on iced guys.
1978 Mar. 25 (18)	USA, Illinois, Argenta	401	209	Overload of heavy ice.
1978 Mar. 26 (9)	USA, Illinois, Bluffs	484	183	Overload of heavy ice.
1979 Dec. 27 (19)	Sweden, Sunne	324	425	Fatigue failure. Wind on lightly iced mast?
1983 (--)	Canada, Manitoba, Brandon	411	--	Overload of heavy ice?
1983 Mar. (--)	Canada, Saskatchewan, Carlyle	207	--	Overload of heavy ice?
1983 Mar. 11 (--)	USA, Maine, Winn Mount	395	--	Ice and wind?
1983 Nov. 28 (15)	USA, Iowa, Rowley	610	298	Overload of ice and wind.
1984 Mar. 18 (2)	USA, Kansas, Colwich	354	425	Heavy ice load or ice shedding?
1984 Mar. 19 (--)	USA, Kansas, Topeka	438	--	Heavy ice load?
1986 Dec. 2 (19)	USA, Nebraska, Bassett	465	770	Overload of heavy ice.
1987 Dec. 26 (24)	USA, Oklahoma, Coweta	582	195	Overload of heavy ice.
1987 Dec. 28 (--)	USA, Oklahoma, Tulsa	579	--	Overload of heavy ice.
1988 Feb. 7 (23)	Sweden, Sollefteå	324	390	Overload of heavy ice and wind.
1989 Dec. 10 (2)	USA, N. Carolina, Auburn	588	120	Dynamic overload due to ice shedding?
1989 Dec. 10 (10)	USA, N. Carolina, Auburn	610	97	Dynamic overload due to ice shedding?
1991 Nov. 1 (5)	USA, Iowa, Woodward	313	305	Overload of ice and wind

1.2 Scope

The theory for modelling atmospheric icing by in-cloud icing is briefly presented in a literature review followed by a discussion on the main results of papers I-IV.

Measurements of icing on a 1m high rod by an ice scale, as well as measurements of air temperature, relative humidity and wind, have been crucial for the success of this work. These measurements have led to the development of a method for estimating liquid water content (LWC) and wind speed in remote areas. These are important parameters for ice accretion by in-cloud icing. In-cloud icing has been found to be the type of icing giving the highest accumulated ice loads. The largest ice-load ever recorded on a power line is 305 kg m^{-1}. This was recorded on a 22 kV overhead line in Voss, Norway on April 18, 1961 (Figure 1.1).

Figure 1.1. Rime on a 22 kV overhead line at Voss, Norway on April 18. 1961. Ice-load recorded was 305 kg m^{-1} on each span. (photo: Olav Wist).

Measurements of ice loads are sparsely reported both in time and space. The use of direct ice load measurement in the design criteria of constructions is rare. A statistically meaningful extreme analysis would require data from several years. Therefore, much attention has been paid to estimate atmospheric ice loads using meteorological data from weather stations (e.g., Haldar et al. 1988; Makkonen and Ahti, 1995; Sundin and Makkonen, 1998; Harstveit, 2002). This approach has the advantage that meteorological data are available for many years with a relatively good spatial coverage.

However, an extrapolation of these data to the site of interest is often necessary.
In this study, measured ice load, icing intensity and duration for a 1m high rod at 10-minute intervals are compared with field weather station data, also at 10-minute intervals. Data from synoptic weather stations are also used as a comparison. The synoptic weather station have measurements, every day, at 0000 hrs, 0600 hrs and 1800 hrs GMT. A method of estimating in-cloud icing by use of weather station data is presented.

1.3 Structure of the report

The report is divided into seven chapters, where the four papers are presented in chapter 4. The papers are not presented at the end of the report due to the fact that the equipment, models and methods evaluated in the papers are applied in chapter 5. The whole report can therefore be read chronologically.

2. Atmospheric accretion

Accretion is defined as the process where ice builds up on the surface of an object. Different types of icing on structures are recognised, and atmospheric icing is traditionally classified according to three different formation processes.

1) Precipitation icing:
    a. freezing rain or drizzle;
    b. accumulation and refreezing of wet snow.
2) In-cloud icing, caused by super-cooled water droplets in clouds or fog.
3) Hoar frost/sublimation. Direct phase transition from water vapour into ice. Hoar frost is of low density and strength, and normally does not result in significant load on structures (Makkonen, 1984a).

The density of the different types of ice is varying from 200 to 900 kg/m^3 (table 2.1).

Table 2.1. Typical properties of accreted atmospheric ice (ISO 12494:2001, 2001).

Type of ice	**Density** kg/m^3	**Adhesion and cohesion**	**General appearance**	
			Colour	**Shape**
Glaze	900	strong	transparent	evenly distributed/icicles
Wet snow	300 to 600	weak (forming) strong (frozen)	white	evenly distributed/eccentric
Hard rime	600 to 900	strong	opaque	eccentric, pointing windward
Soft rime	200 to 600	low to medium	white	eccentric, pointing windward

Ice accretion also depends on the properties of the accreting object itself, described by its shape, size, material and orientation relative to the wind, as well as the surrounding surface structure. Measurements of ice accretions

therefore have to be specified with respect to devices, procedures, arrangements on site, etc.

Accretion by in-cloud icing is the main topic of this study.

2.1 In-cloud icing

Cloud droplets are considerably smaller in size than raindrops, having typical radii of 10 and 1000 microns, respectively.
Within a cloud, the flux density, F, is a product of the mass concentration (cloud liquid water content), ρ_{lwc}, and the wind speed, v, of the cloud droplets relative to the object. Consequently, the rate of icing onto an object with cross-sectional area, A (relative to the direction of the wind speed v), is obtained from

$$\frac{dM}{dt} = \alpha_1 \alpha_2 \alpha_3 \rho_{lwc} vA \qquad (2.1)$$

where α_1, α_2 and α_3 are correction factors that represent processes that may reduce dM/dt from its maximum value. The correction factors vary between 0 and 1. α_1 denotes the collision efficiency, α_2 the sticking efficiency, and α_3 the accretion efficiency.

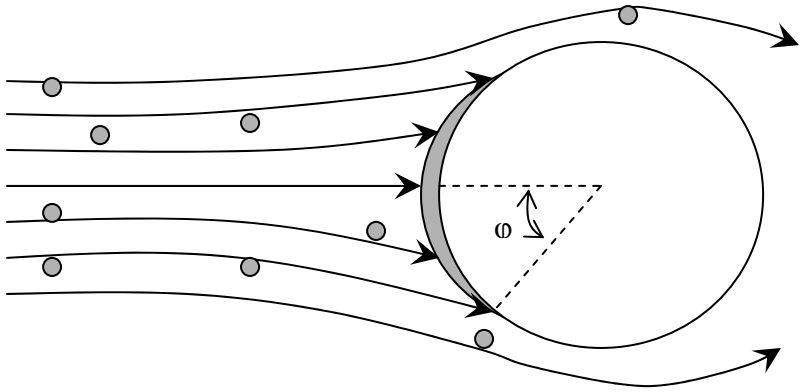

Figure 2.1. Air streamlines of droplet trajectories around a cylindrical object

2.2 Efficiency coefficients

α_1 represents the collision efficiency of the particles, i.e. α_1 is the ratio of the flux density of the particles that hit the object to the maximum flux density. The forces of aerodynamic drag and inertia determine the trajectory of a droplet, moving with the air-stream towards an icing object. Since the air flows around the object, the droplets also tend to do so. The collision

coefficient α_1 becomes less than one when the water droplets follow the streamlines around the object without colliding (figure 2.1). Small droplets, large object and low wind speeds reduce α_1.
Langmuir and Blodgett (1946) performed a theoretical investigation of water droplet trajectories around cylinders. This investigation describes how droplets collide with the cylinder within a band limited by polar angles $-\varphi$ to φ. The angle φ is a function of the droplet radius, cylinder radius, air speed, air temperature and pressure. These calculations are computationally time consuming and complicated. For practical applications simplifications are necessary. Assuming that the icing object is cylindrical, the collision efficiency can be parameterised by the two dimensionless parameters,

$$K = \rho_w \cdot d^2 \cdot v / 9 \cdot \mu \cdot D \tag{2.2}$$

and

$$\phi = \frac{\mathrm{Re}^2}{K} \tag{2.3}$$

where the Reynolds number, Re is given by:

$$\mathrm{Re} = \frac{\rho_a \cdot d \cdot v}{\mu} \tag{2.4}$$

Here v is the free stream velocity, d is the droplet diameter, D is the cylinder diameter, ρ_w is the water density, μ is the absolute viscosity of air, and ρ_a is the air density.

Empirical fit equations to the numerically calculated data for the collision efficiency as a function of median volume droplet diameter (MVD), wind speed and cross sectional area of a cylinder, are given by Finstad et al. (1988a).

$$\alpha_1 = A - 0.028 - C(B - 0.0454) \tag{2.5}$$

where

$$A = 1.066K^{-0.00616}\exp(-1.103K^{-0.688})$$
$$B = 3.641K^{-0.498}\exp(-1.487K^{-0.694})$$
$$C = 0.00637(\phi - 100)^{0.381}$$

Finstad et al. (1998b) have shown that MVD can accurately replace the droplet diameter, d, without having to calculate α_1 individually for each droplet-size category.
Variation of the collision efficiency is considerable with varying wind speed, droplet size and cylinder diameter (figure 2.2).

D

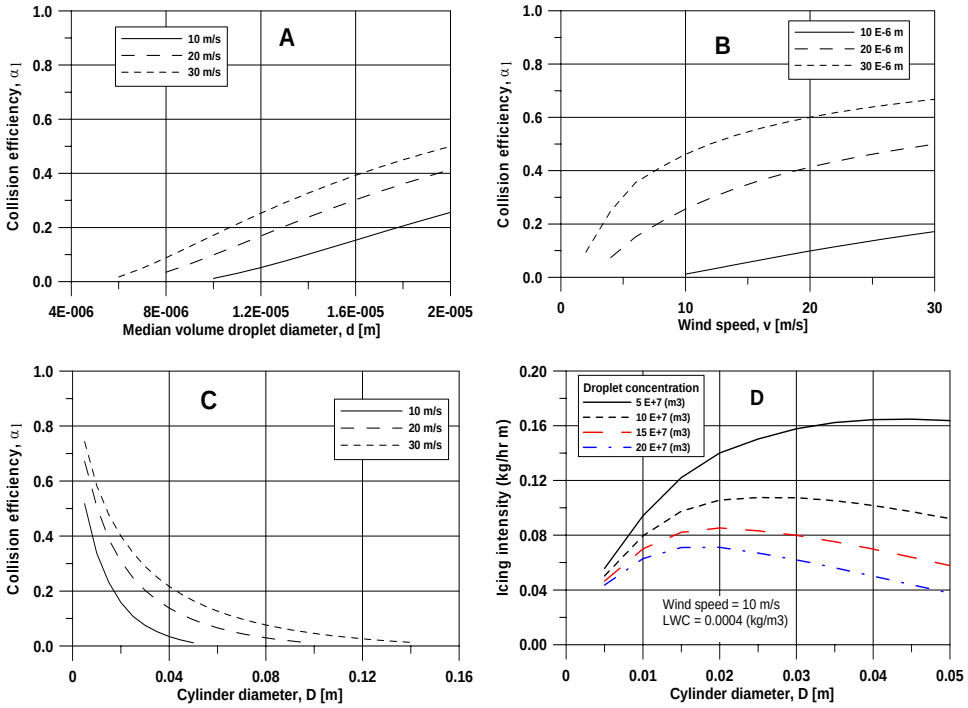

Figure 2.2. A. Collision efficiency, α_1, as a function of MVD at different wind speeds. Cylinder diameter is 30mm. B. Collision efficiency, α_1, as a function of wind speed, v, at different MVD. Cylinder diameter is 30 mm. C. Collision efficiency, α_1, as a function of cylinder diameter, D, at different wind speeds. MVD 13 μm. D. Icing intensity as a function of cylinder diameter, at different droplet concentrations. LWC is taken to be 0.4 g/m3, and wind speed to be 10 m/s. All calculations are based on the equations of Finstad et al. 1988a.

The collision efficiency increases approximately linearly with increasing MVD and wind speed, while it has an exponential decrease with increasing cylinder diameter. More interesting is the variation in calculated icing intensity with varying cylinder diameter. Given a wind speed of 10 m/s, a

LWC of 0.4 g/m3 and a droplet concentration of 10 E+7 m3, a cylinder diameter of 0.03 m has the highest icing intensity according to this calculation method.

α_2 represents the efficiency that an object collects the particles that collide with it, i.e. α_2 is the ratio of the flux density of the particles that stick to the object to the flux density of the particles that hit the object. The collection efficiency, α_2, is reduced from 1 when the particles bounce off the surface. Particles are considered to have stuck either when they are permanently collected or their residence time on a surface is sufficient to affect the icing rate. This happens as a result of the heat exchange between particle and surface, when the particle freezes. The collection efficiency is assumed to be equal to 1 for in-cloud icing (Ahti and Makkonen, 1982).

α_3 represents the efficiency of accretion, i.e. α_3 is the ratio of icing to the flux density of the particles that stick to the surface. Efficiency of accretion reduces from 1 when the heat flux from the accretion is too small to cause sufficient freezing to incorporate all the sticking particles into the accretion. In such a case, part of the mass flux of the particles is lost from the surface by run-off (Makkonen, 1996). At some specific ρ_{LWC} or wind speed the released heat of freezing will increase the surface temperature (T_s) to 0ºC. The minimum value of the ρ_{LWC} , at which T_s reaches 0ºC, is called the Ludlam limit (Ludlam, 1951). The heat balance over an ice surface is given by figure 2.3.

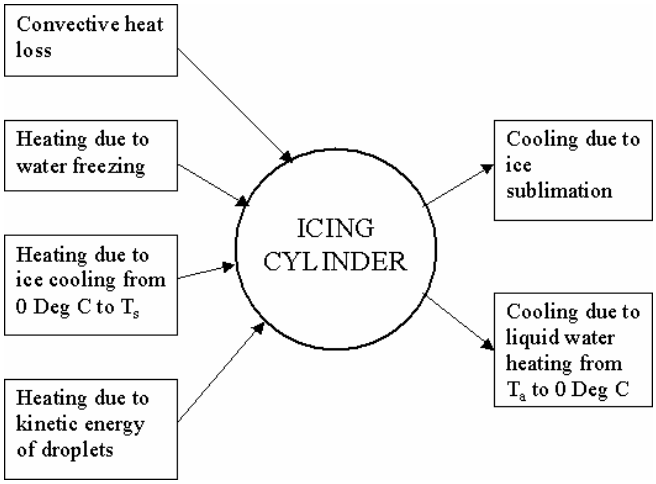

Figure 2.3. The heat balance over an ice surface (Mazin et al., 2001).

T_s can be found iteratively by solving the equation of this heat balance, given by Mazin et al. (2001). The heat budget over the cylinder surface has not been estimated in this study. For LWC >0 and air temperature below 0˚C, the growth process is not assumed to be affected by bouncing and runoff from the accretion surface. Further evaporation and sublimation is not taken into consideration. The main focus has been on estimating growth by in-cloud icing, correlated with collision efficiency, wind speed and LWC.

2.3 Cloud liquid water content

A method for the calculation of the cloud liquid water content (LWC) is outlined in paper 2. Measurements of relative humidity and air temperature at a known level(1) in unsaturated conditions are needed. Based upon the assumption that the total mixing ratio (liquid and vapour) of the air is constant with height, the density, $\rho_{lwc,}$ of LWC (kg/m3) at level z (m a. s. l.) is given by

$$\rho_{lwc}(z) = \varepsilon \cdot \rho_d \left(\frac{e_1}{p_1} - \frac{e(z)}{p(z)} \right) \qquad (2.6)$$

where p is the air pressure, e is the water vapour pressure, and ρ_d is the density of dry air. ε is the constant ratio of the molecular weight for water vapour and dry air, equal to 0.622.

The dry adiabatic temperature gradient, Γ_d, is, by definition, equal to g/c_p, where g is gravitational force, and c_p is specific heat at constant pressure. This gives Γ_d equal to 0.0098ºC/m. Measurements on the mountain Brosviksåta gave a measured temperature gradient for unsaturated conditions equal to 0.0092 ºC/m. The measured temperature gradient for saturated conditions was 0.0062 ºC/m, while the calculated pseudo-adiabatic lapse rate in the temperature range –10ºC to 0 ºC is 0.0067 ºC/m. The LWC increases with height, but with values slightly less than adiabatic. This was expected with regards to previous studies (Adapted from Schemenauer et al., 1980.) (figure 2.4).

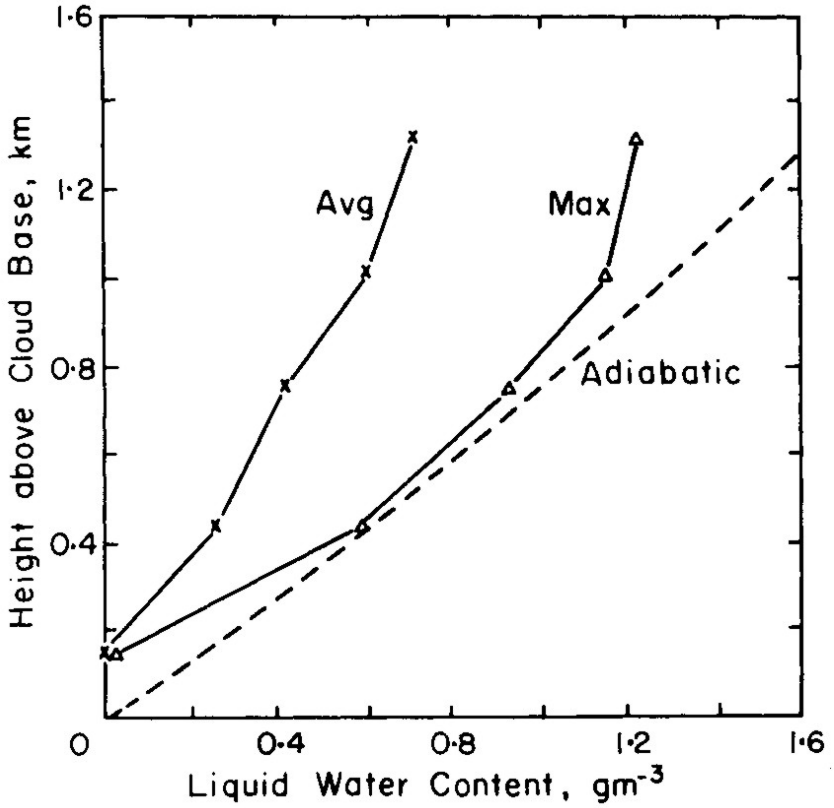

Figure 2.4. Maximum, average, and adiabatic liquid water content plotted against height above cloud base. (Adapted from Schemenauer et al., 1980.)

2.4 Cloud droplet spectrum

Finstad et al. (1988b) show that the median volume droplet size (MVD) is the most suitable parameter for estimating the icing intensity given by equation 2.1. Knowledge of the cloud droplet spectrum is necessary in order to calculate MVD. Measurements of MVD are not a part of routine weather observations, making reliable approximations necessary. However, given that LWC and droplet concentration are known, the mean volume droplet size, D_{mv}, is easily calculated by the equation

$$D_{mv} = \left(\frac{6}{\pi} \frac{V}{N} \right)^{1/3} \tag{2.7}$$

where V is the total volume of cloud liquid water, and N is the droplet concentration.

In most cases the use of mean volume droplet size will lead to an underestimate of the in-cloud icing intensity, due to the fact that the mean volume droplet size is smaller than the MVD. Finstad et al. (1988b) compares MVD and mean volume droplet size with collision efficiency, based on droplet size data either measured in the field, in icing wind tunnels or estimated from parameterised size distribution. The data were collected from 1957 to 1987 (table 2.2). A comparison of MVD with mean volume droplet sizes, based on their results, is presented in figure 2.5. This result gives a method of estimating MVD based on mean volume droplet size. Applying a linear fit, MVD is a function of mean volume droplet diameter given by the equation

$$MVD = 1.49 \cdot D_{mv} + 0.56 \qquad (2.8)$$

where D_{mv} is mean volume droplet diameter.

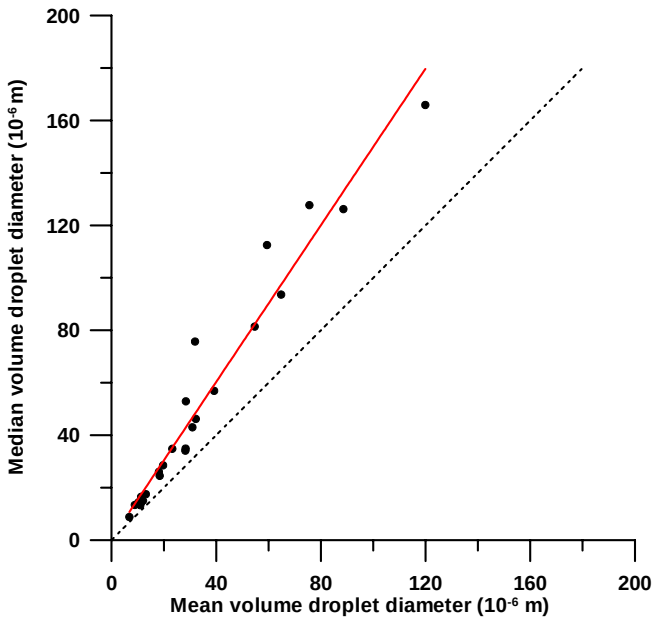

Figure 2.5. Mean volume droplet size plotted against median volume droplet size. Empirical fit (solid line) and 1:1 line (dotted line) are also plotted. The droplet size data is either measured in the field, or in icing wind tunnels, or estimated from empirical size distributions, during the period 1957 to 1987.

Table 2.2. Different measurements/estimates of cloud droplet spectra. (Adapted from Finstad et al. 1988b)

Spectrum	Reference	Source
1	Bain and Gayet (1982)	natural cloud
2	Bain and Gayet (1982)	
3	Bain and Gayet (1982)	
4	Battan and Reitan (1957)	natural cloud
5	Battan and Reitan (1957)	
6	Choularton et al. (1986)	natural cloud
7	Choularton et al. (1986)	
8	University of Alberta, unpublished data	wind-tunnel
9	University of Alberta, unpublished data	
10	University of Alberta, unpublished data	
11	University of Alberta, unpublished data	
12	University of Alberta, unpublished data	
13	Khrgian-Mazin, as in Pruppacher and Klett (1980)	parameterization
14	Khrgian-Mazin, as in Pruppacher and Klett (1980)	
15	Khrgian-Mazin, as in Pruppacher and Klett (1980)	
16	Khrgian-Mazin, as in Pruppacher and Klett (1980)	
17	McComber and Touzot (1981)	wind-tunnel
18	McComber, personal communication	wind-tunnel
19	Makkonen and Stallabrass (1987)	wind-tunnel
20	Makkonen and Stallabrass (1987)	
21	Makkonen and Stallabrass (1987)	
22	Preobrazhenskii (1973)	natural sea-spray
23	Prodi et al. (1986)	wind-tunnel
24	Prodi et al. (1986)	
25	Squires (1958)	natural cloud
26	Squires (1958)	
27	Squires (1958)	

In this case study, the droplet concentration was assumed to be constant throughout a cloud layer. The cloud droplet number used is 113 cm^{-1}, given by Gjessing and Skartveit (1990). The literature shows convincing evidence that, at higher altitudes, the droplet spectrum shifts to larger sizes (Schemenauer et al., 1980, Nicholls, 1984, Noonkester, 1984). They show that in the middle and upper portion of the cloud, the droplet concentration decreases with increasing altitude. However, the increase in droplet size due to decreasing droplet concentration is small compared to the increase in droplet size due to increasing LWC with height. Therefore, we ignore the growth in droplet size by coalescence processes, and consider condensation as being the only process leading to the growth of droplets.

A droplet that forms on a large condensation nucleus is initially seen to grow at a faster rate than droplets with small nuclei, but after reaching a certain radius, the growth rates equal out, regardless of nuclear mass. Furthermore, the droplet radius, r, increases with time according to

$$r(t) = \sqrt{r_0^2 + 2\xi \cdot t} \tag{2.9}$$

where r_0 is initial radius and ξ is given by

$$\xi = (S-1)/(F_k + F_d) \tag{2.10}$$

where S is ambient saturation ratio, F_k is the thermodynamic term associated with heat conduction, and F_d is the term associated with vapour diffusion.

Parcels of dry air are mixed into the cloud layer by entrainment at the cloud top. The exact nature of this process and the evolution of the droplet size distribution are still debated issues. The theory for estimating LWC presented here is, therefore, not assumed to be valid in this transition layer. The cloud top is, therefore, assumed to be above the site of interest where we are measuring and estimating icing.

2.4.1 Multicylinder measurements

The multi-cylinder method has proven successful in measuring cloud droplet size and liquid water content (Makkonen, 1992). This system contains of a set of cylinders of different diameters, which rotates at a frequency of 0.2 Hz (figure x). The dimension and weight of the accreted ice is measured after a given time interval, which depends upon icing intensity. High icing intensity requires a short measurement interval.

The rotating multi-cylinder method was applied during the field experiments between March 28 and April 2, 2003. The cylinders used had an initial diameter of 1, 5, 10, 20, 50 and 80 mm. The weight and dimension of the accretions on the separate cylinders was measured after an icing interval of 20 minutes. The accuracy of the scale used for these measurements was estimated to ± 0.1 g. A program given by Finstad (personal communication) developed to calculate the median volume droplet size (MVD) and LWC based on these measurements was applied. The input parameters in the model are dimension (length and width) of the ice accretion on each cylinder, the wind speed, the air temperature and the duration of the icing incident. The reliability of the calculations by this method has been thoroughly tested and verified (Makkonen, 1992).

Due to inaccuracies in the wind speed measurements, calculations were made for varying wind speed at the different cases to illustrate the dependence upon wind speed (Table 1 and 2). Further, the mean volume droplet size and droplet concentration are estimated according eq. 2.7 and 2.8. These estimates indicate a higher droplet concentration than 113 (cm^{-3}). However, the variation is relatively high, from 531 to 1770 (cm^{-3}) in case 1, and from 291 to 1290 in case 2. A droplet concentration of 113 (cm^{-3}) is therefore possibly to low. However, the concentration is kept constant equal 113 (cm^{-3}) in this study due to the high inaccuracies and variations in droplet concentration according the multicylinder experiments (table 1 and 2). A further study on the droplet concentration is preferred to investigate the variation in space and time of droplet concentration.

Table 1. Case 1: Calculated LWC (kg/m^3) and MVD (m) by the multicylinder method at Gaustatoppen March 29 2003.

29.03.2003	Wind speed (m/s)	LWC (kg/m3)	MVD (m)	Mean volume droplet size (m)	Droplet concentration (cm-3)
1200:1220 hrs	12	2,30E-04	8,40E-06	5,41E-06	7,41E+08
	15	1,80E-04	7,70E-06	4,92E-06	7,53E+08
	18	1,80E-04	5,80E-06	3,61E-06	1,76E+09
1225:1245 hrs	12	3,20E-04	8,80E-06	5,68E-06	8,97E+08
	15	2,60E-04	7,80E-06	4,99E-06	1,05E+09
	18	2,20E-04	7,20E-06	4,58E-06	1,13E+09
1245:1305 hrs	12	6,40E-04	9,60E-06	6,23E-06	1,38E+09
	15	5,10E-04	8,70E-06	5,61E-06	1,48E+09
	18	4,40E-04	7,80E-06	4,99E-06	1,77E+09
1305:1325 hrs	12	3,60E-04	1,04E-05	6,79E-06	6,11E+08
	15	2,90E-04	9,30E-06	6,03E-06	6,89E+08
	18	2,50E-04	8,40E-06	5,41E-06	8,06E+08
1325:1345 hrs	12	4,50E-04	8,70E-06	5,61E-06	1,31E+09
	15	3,70E-04	7,80E-06	4,99E-06	1,49E+09
	18	3,10E-04	7,20E-06	4,58E-06	1,59E+09
1350:1410 hrs	12	3,50E-04	1,08E-05	7,06E-06	5,31E+08
	15	2,80E-04	9,70E-06	6,30E-06	5,86E+08
	18	2,30E-04	9,10E-06	5,89E-06	5,83E+08
1410:14:30 hrs	12	4,00E-04	9,50E-06	6,17E-06	8,91E+08
	15	3,20E-04	8,60E-06	5,54E-06	9,61E+08
	18	2,70E-04	7,90E-06	5,06E-06	1,05E+09
1435:14:55 hrs	12	2,40E-04	8,30E-06	5,34E-06	8,02E+08
	15	1,90E-04	7,50E-06	4,79E-06	8,60E+08
	18	1,60E-04	6,90E-06	4,37E-06	9,30E+08

Table 2. Case 2: Calculated LWC (kg/m^3) and MVD (m) by the multicylinder method at Gaustatoppen April 01 2003.

01.04.2003	Wind speed (m/s)	LWC (kg/m3)	MVD (m)	Mean volume droplet size (m)	Droplet concentration (cm-3)
1030:1050 hrs	13	5,80E-04	1,43E-05	9,48E-06	3,79E+08
	16	4,70E-04	1,30E-05	8,58E-06	4,09E+08
	19	3,90E-04	1,24E-05	8,17E-06	3,91E+08
1055:1115 hrs	13	8,60E-04	1,14E-05	7,48E-06	1,11E+09
	16	7,00E-04	1,04E-05	6,79E-06	1,19E+09
	19	5,90E-04	9,60E-06	6,23E-06	1,27E+09
1120:1140 hrs	13	5,60E-04	1,39E-05	9,20E-06	3,98E+08
	16	4,60E-04	1,27E-05	8,37E-06	4,29E+08
	19	3,80E-04	1,21E-05	7,96E-06	4,10E+08
1145:1205 hrs	13	6,88E-04	1,20E-05	7,89E-06	7,60E+08
	16	5,50E-04	1,10E-05	7,20E-06	7,89E+08
	19	4,60E-04	1,03E-05	6,72E-06	8,04E+08
210:1230 hrs	13	4,90E-04	1,35E-05	8,92E-06	3,80E+08
	16	4,00E-04	1,23E-05	8,10E-06	4,11E+08
	19	3,40E-04	1,13E-05	7,41E-06	4,50E+08
1235:1255 hrs	13	5,10E-04	1,37E-05	9,06E-06	3,79E+08
	16	4,20E-04	1,24E-05	8,17E-06	4,21E+08
	19	3,50E-04	1,17E-05	7,68E-06	4,17E+08
1300:1320 hrs	13	4,80E-04	1,32E-05	8,72E-06	3,99E+08
	16	3,80E-04	1,30E-05	8,58E-06	3,30E+08
	19	3,20E-04	1,28E-05	8,44E-06	2,91E+08

3. The experiments

3.1 Field site

The field data presented in this study was collected at two different mountain sites in Norway. The two sites were Brosviksåta (723 m a.s.l., 61˚ 2` N, 5˚ 9`E) and Gaustatoppen (1883 m a. s. l. 59˚ 51`N, 8˚ 39`E). Brosviksåta is situated on the western coast, while Gaustatoppen is situated inland in the southern part of Norway (figure 3.1). Daily weather conditions along the Norwegian coast are primarily dominated by large-scale synoptic systems moving in from the west. Such systems result in several periods of icing during the winter months. Brosviksåta experiences rather short periods of icing (days) both as precipitation icing and in-cloud icing, while the height of Gaustatoppen is favourable for long periods (weeks) of extreme in-cloud icing. In addition to the well-suited climatic conditions, the infrastructure at both sites makes them ideal for experimental activity. Brosviksåta has a road all the way to the top, while Gaustatoppen has an elevator inside the mountain from 1150 to 1800 m a.s.l. Nevertheless, a key factor for the success of these experimental studies has been the excellent support given by the operating personnel at both sites.

The main purpose of the experiments was to collect full-scale data of the meteorological parameters relevant for atmospheric icing and, at the same time, measure the icing intensity with suitable equipment. Air temperature, relative humidity, wind speed and wind direction have been measured at different levels along the mountain slope. At the same time, the icing intensity was measured at the mountain peak by an ice scale (Figure 3.2). All equipment made samplings at 10-minute intervals.

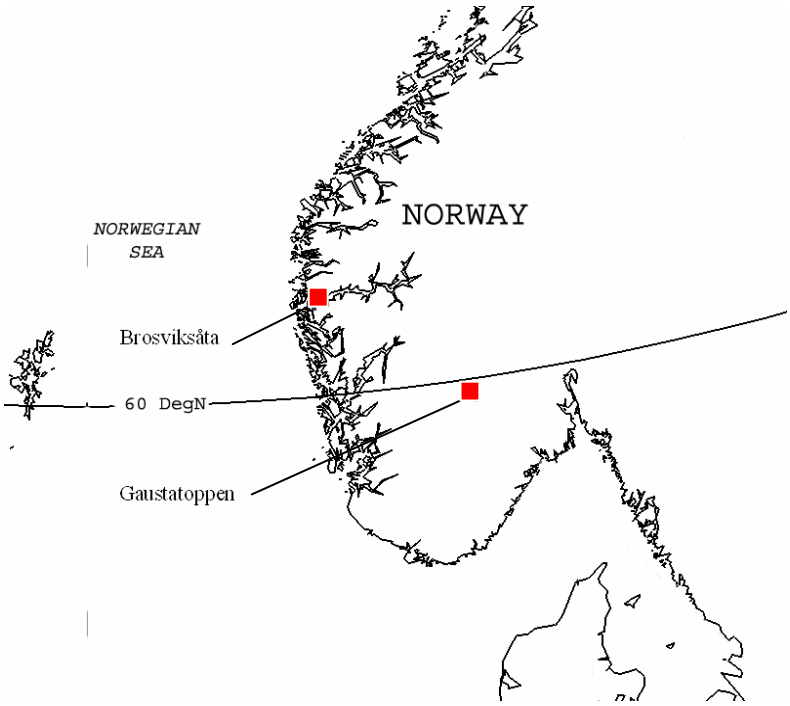

Figure 3.1. Location of the mountains Gaustatoppen (59º51´N, 08º39´E) and Brosviksåta (723 m a.s.l., 61º 2` N, 5º 9` E).

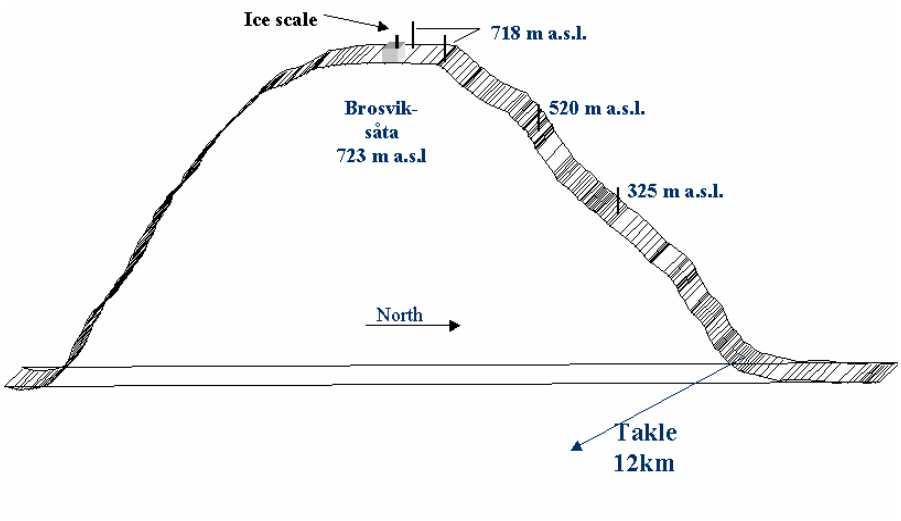

Figure 3.2a. Schematic drawing of the measurement set-up at Brosviksåta (723 m a.s.l.). Two weather stations were placed at 718 m a.s.l.,one at 520 and one at 325 m a.s.l. The ice scale was mounted on the roof of a building at the top of the mountain. The station Takle is situated 12 km east of the base of the mountain.

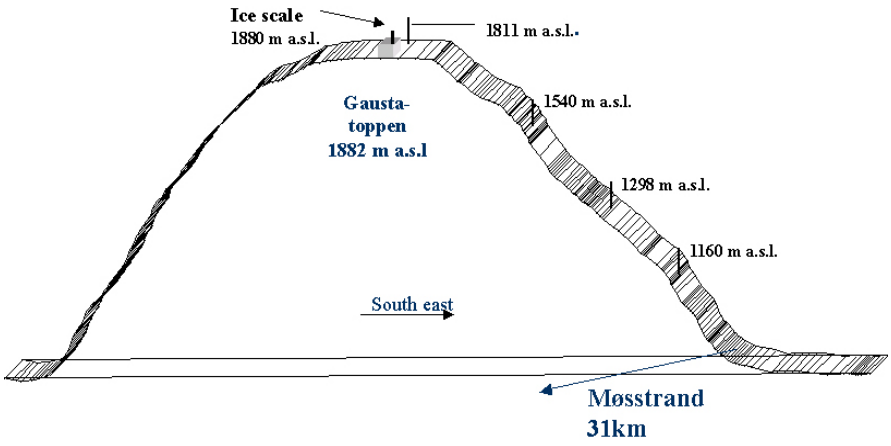

Figure 3.2b. Schematic drawing of the measurement set-up at Gaustatoppen (1882 m a.s.l.). The weather stations were placed at 1811, 1540, 1298 and 1160 m a.s.l. The ice scale was mounted 3 m above the terrain at 1800 m a.s.l.. The synoptic weather station Møsstrand is situated 31 km southwest of the mountain.

3.2 Meteorological instrumentation

Dipl. Ing Houm and Aanderaa Instruments, Norway, manufactured the meteorological instruments used in this study. The sensors were integrated in a system consisting of sensors, a sensor-scanning unit, a power supply and a data storage unit. The system has been extensively tested over several years, giving satisfactory results for non-icing conditions. The performances of the wind velocity and wind direction sensors were tested

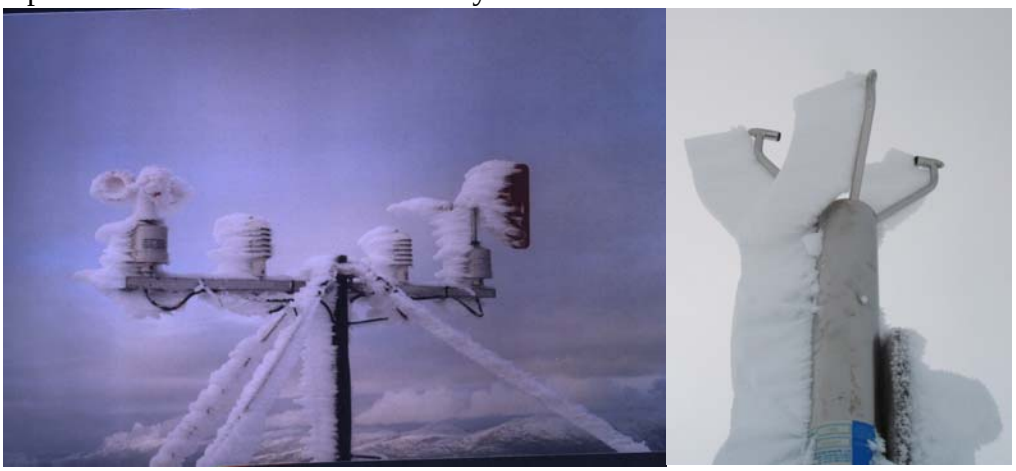

Figure 3.3. Iced Aandera weather station at Brosviksåta March 23, 2004 (left), and iced Gill Windobserver II at Gaustatoppen February 26 2002 (right) (photo: Tor de

against other sensor types by Aasen (1995). Each weather station along the slope of the mountain consisted of a range of these sensors. A heated acoustic anemometer (from Gill Instruments) was mounted together with the ice scale at the mountain peak. All instrumentation for measuring atmospheric icing is described in detail in paper 1 (Drage and de Lange, 2005).

The wind speed and wind direction sensors from Aanderaa Instruments were not suitable for operation under icing conditions. The acoustic anemometer has a heating element to keep the senor arms free of ice. This heating proved to be insufficient during heavy icing conditions (figure 3.3). A procedure for calculating the wind speed at the site of interest, based on measurements at a lower level and by use of operational model data (HIRLAM10 (High Resolution Medium range Weather Forecast), ECMWF (European Centre of Medium range Weather Forecasts), was therefore more appropriate.

3.3 Ice scale

For measuring atmospheric icing, a system was constructed based on the requirements outlined in ISO 12494 (2001). The entire measurement system is described in detail in paper 1. The ice scale system consists of the following main components: ice scale, data logger, power-supply and converter units.

4. Papers

4.1 Specific objectives of the four individual studies

The specific objectives of the four individual studies are presented below, followed by the full version of the papers.

Paper I: Instrumentation for Measuring Atmospheric Icing
The paper is concerned with the design, construction and testing of instrumentation for measuring atmospheric icing. An ice scale, to measure icing, is constructed according to the requirements and specifications outlined in ISO 12494 (2001). The ice scale consists of a vertical steel rod with a length of one meter exposed to atmospheric icing. A load cell records the vertical and horizontal load at 10-minute intervals. The equipment is tested and calibrated under controlled conditions in a laboratory.

Paper II: Atmospheric Icing in a Coastal Mountainous Terrain. Measurements and Numerical Simulations, a Case Study
Development of a method for estimating vertical gradient of cloud liquid water content (LWC), from air temperature and humidity at unsaturated conditions (in respect to water vapour) below the cloud base. A case study of icing is evaluated, where measured icing intensity is compared to estimates from weather station data and numerical simulations. The height of the cloud base is estimated, and temperature at the site of interest inside the cloud is found by following an unsaturated gradient below the cloud base, and a saturated gradient inside the cloud. The total mixing ratio (vapour and liquid) is assumed constant throughout the cloud layer.

Paper III: Large Scale Measurements and Numerical Simulations of In-cloud Icing Around the Ridge of a Mountain Peak
A study of local icing variations in the surface layer around the edge of a mountain ridge has been carried out. Icing is measured in-situ on 16 sticks with a height of 2 meters and a diameter of 30 mm, for measurements of the local variation in icing around the south-eastern part of the ridge at Gaustatoppen (1883 m a.s.l.), Norway. The method outlined in paper II is used for calculating variation in LWC with height. Furthermore, a numerical model, “Flow 3d”, is used for estimating wind speeds 2 m above the ground. A comparison of icing intensity by in-situ measurements and numerical simulations is performed.

Paper IV: Arctic Coastal Climatic Impact on Design Construction and Operation of the Hammerfest LNG Plant

An approach for the evaluation of climatic aspects in relation to design, construction and operation of a plant in an artic coastal area is presented. The focus on exploitation of oil and gas resources in the artic sea and coastal regions requires attention to be paid to climatic aspects. Events such as heavy sea spray icing and snowdrift must be considered. Fast developing, unpredicted polar lows with high wind speeds and heavy precipitation is another design criterion. Design, construction and operation of the LNG (liquid natural gas) plant on Melkøya, Hammerfest, Norway, with respect to climatic conditions are presented in this paper.

5. Testing of models

The last part of this study is concerned with the testing of the models presented in papers 2 and 3. Ice load data collected at Mt. Brosviksåta and Mt. Gaustatoppen during the winter 2003/2004 is evaluated.

5.1 Brosviksåta

At Brosviksåta data were continuously recorded between October 10, 2003 and May 1, 2004, and several incidents of icing occurred (figure 5.1). The ice scale was mounted with a 14 cm diameter one-meter high non-rotating rod during the period October 7, 2003 to February 23, 2004. On February 23, 2004, a rotating cylinder of 3 cm diameter replaced the 14 cm cylinder. For all cases, the ice was assumed to have fallen off when the air temperature was higher or equal to 0 ºC.

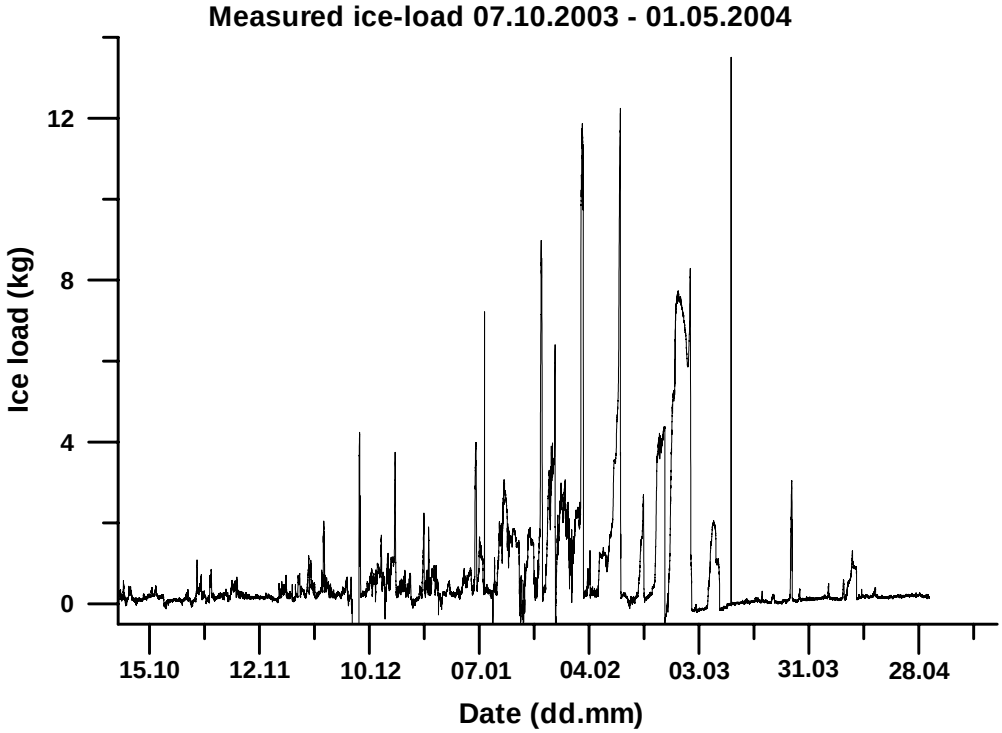

Figure 5.1: Recorded ice load on a one-meter high rod at Brosviksåta 723 ma a.s.l. during the period October 10, 2003 to May 1, 2004.

5.1.1 Non-rotating cylinder

A non-rotating rod was chosen due to the fact that most constructions like masts, buildings, antennas etc. are rigid. Equations for calculation of collision efficiency with a cylinder are given by Finstad et al. (1988a) and are therefore generally not applicable in these cases. In theory, the ice is supposed to create a vane on the windward side of a non-rotating cylinder, which was confirmed by inspection on February 23, 2004. The shape and direction of the vane is strongly dependent upon variations of the wind direction. Brosviksåta, which is situated on the coast, experiences a high variation in air temperature, wind speed, wind direction, precipitation rate and humidity. The incidents of icing are however of relatively short duration (days), due to the fact that the air temperature often rises above 0 ºC at the end of an icing incident. As a result, the ice then falls off.

Examination of the different icing incidents with the non-rotating cylinder shows that the wind direction is stabile during any given icing incident within an interval of ±15 degrees.

The width of the ice vane decreases as the ice forms, creating a peak pointing towards the wind. This can be interpreted physically as a decreasing effective cylinder diameter as the ice continues to form. The theoretical calculation of change in collision efficiency with varying cylinder diameter is given in figure 2.2 in chapter 2. Given a wind speed of 10 m/s, a LWC of 0.4 g/m^3 and a droplet concentration of 100 pr/m^3, this figure shows that the icing intensity (kg/m hr) has a maximum when the cylinder diameter is approximately 3 cm, decreasing rapidly with decreasing cylinder diameter and decreasing slowly with increasing cylinder diameter. Assuming a constant diameter of 14 cm, the collision coefficient variations are a function of wind speed, LWC and droplet concentration. During an in-cloud icing incident with only minor changes in wind direction, the width of the ice vane will decrease. Thus, an underestimate of icing is expected until the width of the ice vane decreases towards the critical diameter given by figure 2.2. An overestimate should be expected when the wind direction changes during an icing incident.

5.1.2 Methods

LWC is estimated by the method described in the introduction and also in detail in Drage and Hauge (2004) (paper 2). For a fixed diameter of the cylinder, and assuming a constant droplet number of 113 drp/m^3, the icing intensity will vary as a function of LWC and wind speed. For a constant droplet concentration, an increase in wind speed or LWC will both lead to an increase in collision efficiency, according to the theory by Finstad et al.

(1988a) (figure 2.2). In the following three methods for ice-load estimates are outlined.

Method 1:
Wind speed, droplet concentration, droplet size (Median Volume Droplet) and the dimensions of the icing object, all control the collision efficiency. Assuming constant droplet concentration and object dimensions, wind speed and droplet size are the controlling parameters. For a constant droplet concentration, the MVD is only a function of LWC.
A simple approach for calculating the collision efficiency might be expressed by the formula

$$\alpha = k_1 \cdot \rho_{LWC} \cdot v \qquad (5.1)$$

where α is the collision efficiency, k_1 is a constant (g/m^2s), ρ_{LWC} is the liquid water content (g/m^3) and v is the wind speed (m/s). In this model the collision coefficient increases linearly with increasing wind speed and/or LWC. An increase of LWC or wind speed by a factor of two will similarly increase the collision coefficient by a factor of two. This is a slight overestimate compared with the theoretical method of Finstad et al. (1988a). The constant k_1 is adjusted to give the best fit against the measured icing at Brosviksåta during the winter 2003/2004, and was found equal to 0.0225 (g/m^2s).

Method 2:
Evaluation of an icing incident at Brosviksåta March 20-25 2003 by Drage and Hauge (paper 2) gave a collision efficiency dependent only on LWC:

$$\alpha = k_2 \cdot \rho_{LWC} \qquad (5.2)$$

where α is the collision efficiency, k_2 is a constant (m^3/g), and ρ_{LWC} is the liquid water content (g/m^3). On this occasion, the best-fit constant, k_2, was found equal to 0.225. Evaluation of data for the winter 2003-2004 gave a k equal to 0.255 (m^3/g), an increase of 13.3 % from the value found in paper 2.

Method 3:
An approach to the problem of estimating in-cloud icing on a non-rotating cylinder, is to assume that it is still a cylinder but that the cylinder diameter is decreasing as a function of accumulated ice. The width of the ice vane decreases with increasing ice load, when wind direction is assumed to be approximately constant during the icing incident. This method is not applicable if the wind direction changes during the icing incident.

Measurements of the width and weight of the ice vane on the 14 cm diameter cylinder on Brosviksåta February 23, 2004, and on the 3 cm diameter cylinders at Gaustatoppen April 1, 2003 are presented in figure 5.2. At Brosviksåta the accumulated ice load on the 14 cm diameter cylinder was 4 kg, while the width of the vane was 10 cm at cylinder surface and 3 cm at the tip of the vane. At Gaustatoppen the accumulated ice load on the 3 cm diameter stick was approximately 4 kg, while the width of the vane was 3 cm at the cylinder surface and 2 cm at the tip of the vane. Based on this the ice vane at Brosviksåta is assumed a further ice growth from 4 to 8 kg and at the same time a decrease in the width of the vane from 3 to 2 cm (figure 5.2).

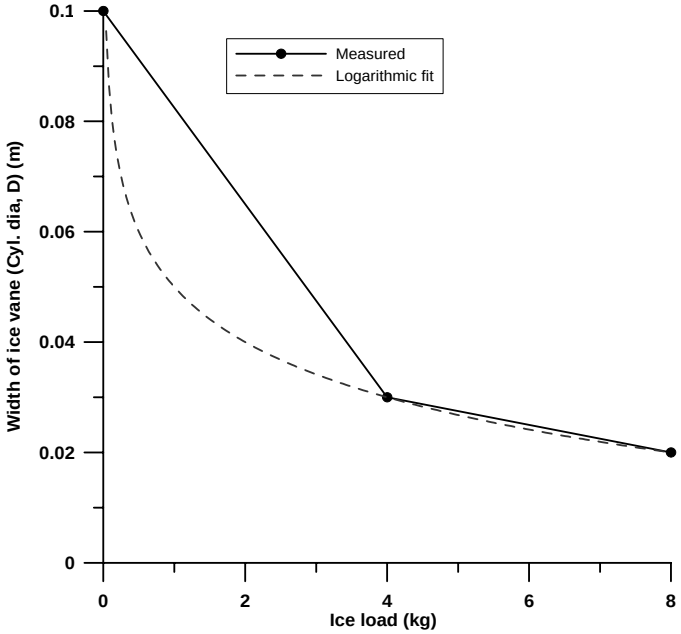

Figure 5.2. Measured width of ice vane (labels) and a best logarithmic fit (dotted line), based on measurements at Brosviksåta and Gaustatoppen

A best-fit logarithmic function is given as

$$D = -1.44 \cdot \ln(x) + 5 \qquad (5.3)$$

where D is the width of the ice vane, and x is ice load in kilograms. Applying the equations given by Finstad et al. (1988a) will result in a negative collision coefficient for large cylinder diameters. This is obviously wrong and a minimum value of 0.01 is therefore chosen, according to Harstveit (2002). An iteration procedure recalculates the cylinder diameter and accumulated ice at each sampling interval.

5.1.3 Model results

Figure 5.3 presents observed ice-loads and ice loads estimated by the three methods described above.

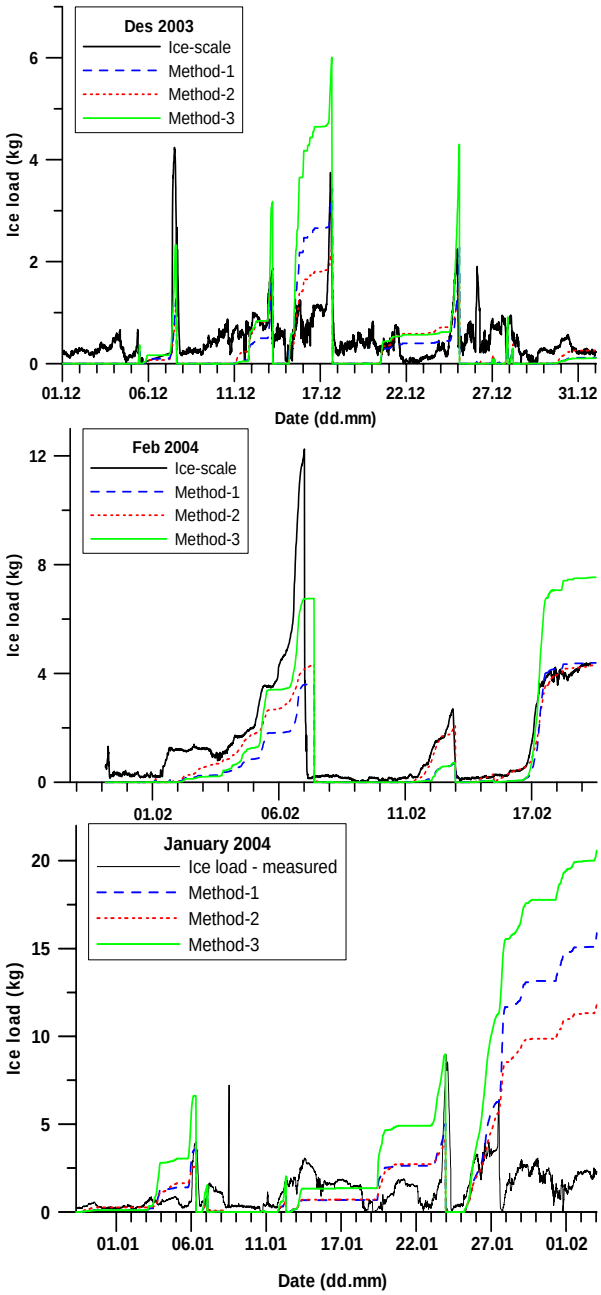

Figure 5.3. Measured and simulated ice load on a one meter high 14 cm diameter non-rotating cylinder at Brosviksåta at 723 m a.s.l. from December to February 2003/2004.

Comparison the results of three methods presented in figure 5.3, indicates that method 2 gives the best result. Method 1 is sometime overestimating and sometime underestimating the ice growth. This can be explained by the relatively high standard deviation in the wind speed ratio. Icing onto the wind speed sensor at the lowest level result in an underestimate of the ice growth.

Calculated collision efficiency in method 2 is independent of wind speed. This method is estimating the ice growth better than method 1. A simple explanation is that the wind speed is relatively constant during an icing incident, and is therefore not affecting the collision efficiency.

Method 3 is generally overestimating the ice growth. An adjustment of the method of decreasing ice vane width is probably needed for a better fit.

5.1.4 Rotating cylinder

The 3 cm cylinder rotates freely. Free rotation means the rod will turn until minimum drag is achieved, creating a cylindrical shape of ice accretion. Several field observations confirm this theory, showing a cylindrical ice accretion on the cylinder (Drage and Lange, 2004) (paper 1). The diameter of the cylinder, D, increases with increasing ice load, and is by geometry given by the formula

$$D = 2 \cdot \sqrt{\frac{m}{\rho_i \cdot h \cdot \pi} + r_c^{\,2}} \qquad (5.4)$$

where m is the mass of ice in kilograms, ρ_i is the density of ice, h is the length of the cylinder, and r_c is the radius of the initial cylinder without ice. The type of ice by in-cloud icing is assumed to be a combination of soft and hard rime, dependent upon wind speed, air temperature and LWC during the icing incident. Calculation of density based upon measurements of size, shape and weight on March 23, 2004, gave a density equal to 500 kg/m^3. The collision efficiency was calculated according to the equations given by Finstad et al. (1988a). Here, measurements of wind speed, relative humidity and air temperature are sampled every 10 minutes at a known level below cloud base. The amount of ice accreted on the cylinder during a 10-minute period is calculated. This amount of ice is added to the total amount of ice, and a new cylinder diameter, D, is calculated. The new cylinder diameter, D, is then used to recalculate the collision efficiency used in the next 10 minute period. This procedure was repeated during the whole measurement period with the 3.0 cm rotating rod, from February 23 to May 1, 2004 (figure 5.4).

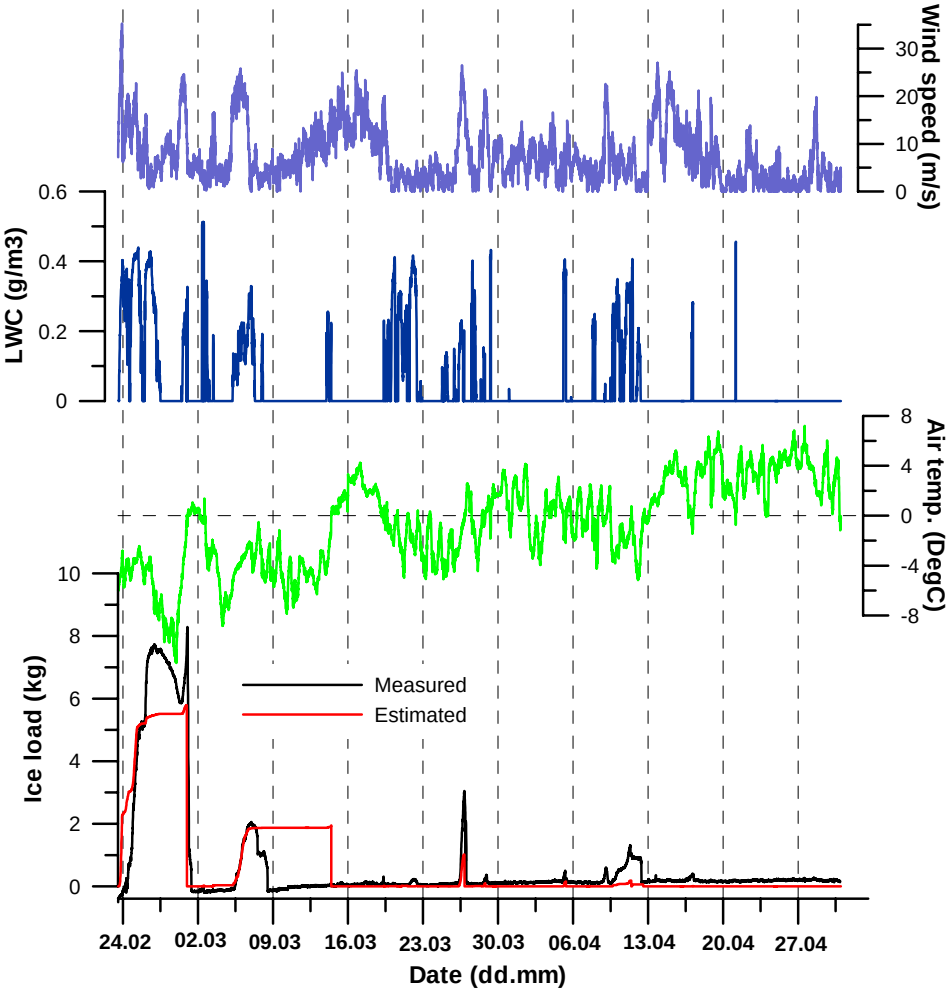

Figure 5.4. Estimated wind speed (m/s), LWC (g/m^3) and air temperature (°C) plotted together with measured and simulated ice load on a one meter high 3 cm rotating rod at Brosvisåta 723 m a.s.l. from February 24, to May 05, 2004.

5.1.5 Assumptions and sensitivity tests

LWC is calculated by equation 2.6 (chapet 2), assuming that the actual site of interest is above the cloud base. When the height of the cloud base is above the height of interest, this results in a negative LWC, which is simply replaced by a LWC equal to zero. A plot of the two independently estimated

and measured parameters, cloud base height and relative humidity, at the mountain top Brosviksåta in January 2004, indicates a negative correlation (figure 5.5). The plot shows that for cloud base above the mountain top, the relative humidity increases as the cloud base lowers, and vice versa. A statistical correlation of these two parameters, from October 07, 2003 to May 01, 2004, gives a correlation coefficient equal to –0.90.

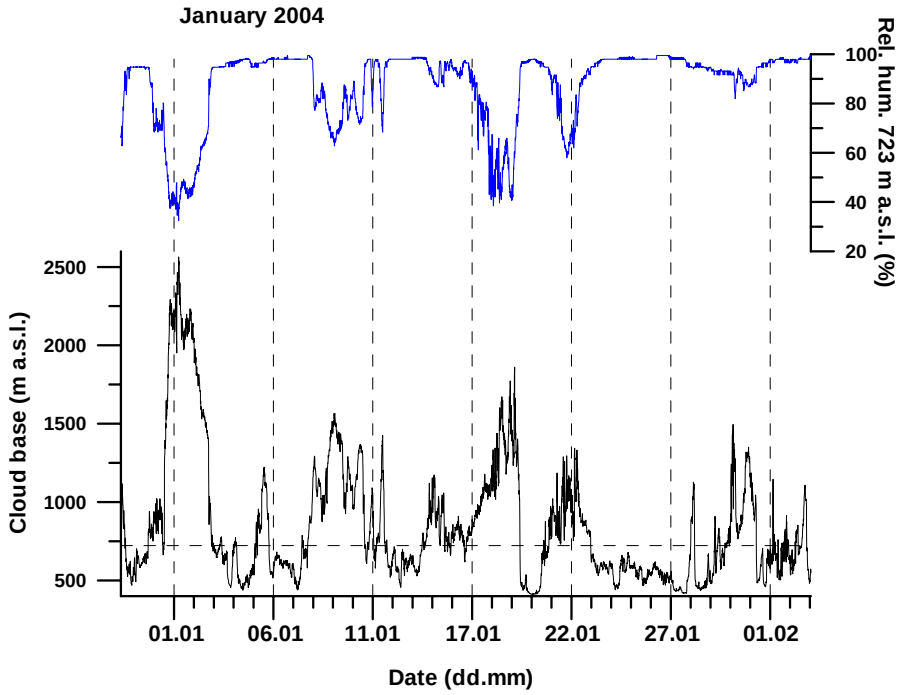

Figure 5.5. Measured relative humidity (%) at 723 m a.s.l. at Brosviksåta plotted against estimated cloud base height, during January 2004.

Variations in wind speed, droplet concentration and ice density are tested to evaluate the effect on estimated ice load. Among these three parameters, the most uncertain one is droplet concentration. A droplet concentration of 113 pr/cm3 was successfully used during a field experiment in eastern Norway (Gjessing and Skartveit, 1990).

A. Wind speed

On Brosviksåta, the wind speed at 723 m a.s.l., is, on average, higher than at 325 m a.s.l. by a factor of 2.2 (paper 2). Three cases of ice load have been estimated using a wind speed ratio of 1.4, 2.2 and 3.0 (figure 5.6). The ratio of 1.4 gives 40%, while the ratio 3.0 gives 179%, of the ice load given by using wind ratio 2.2. Compared with field measurements, the best ice load estimates appeared using wind speed ratio of 2.2.

B. Ice density

The ice density was measured equal to 500 kg/m^3 at February 23, 2004. Variations in ice density result in variations in cylinder diameter, which thereby affects the collision efficiency. Three cases of ice load have been estimated using a ice density of 200, 500 and 800 kg/m3 (figure 5.6). An ice density of 200 kg/m^3 gives 77%, while an ice density of 800 kg/m^3 gives 104%, of the ice load using ice density 500 kg/m3. The figure indicates that at Brosviksåta, a density of 200 kg/m^3 is too low, while a change in density from 500 to 800 kg/m^3 gave only a minor change in ice load.

C. Droplet concentration

A droplet concentration of 113 pr/cm^3 is assumed a good estimate in lack of more field observations. It is regularly used to calculate droplet size, and thereby collision coefficient (Harstveit, 2002). Three cases of ice load are estimated using a droplet concentration of 73, 113 and 153 droplets m^{-3} (figure5.6). A droplet concentration of 73 m^{-3} gives 143%, while a droplet concentration of 153 m^{-3} gives 78%, of the ice load using a droplet concentration of 113 m^{-3}. More interesting here is the fact that a droplet concentration of 73 m^{-3} is a better match to the measured results. A droplet concentration of 113 m^{-3} might be an overestimate for the average conditions on Brosviksåta.

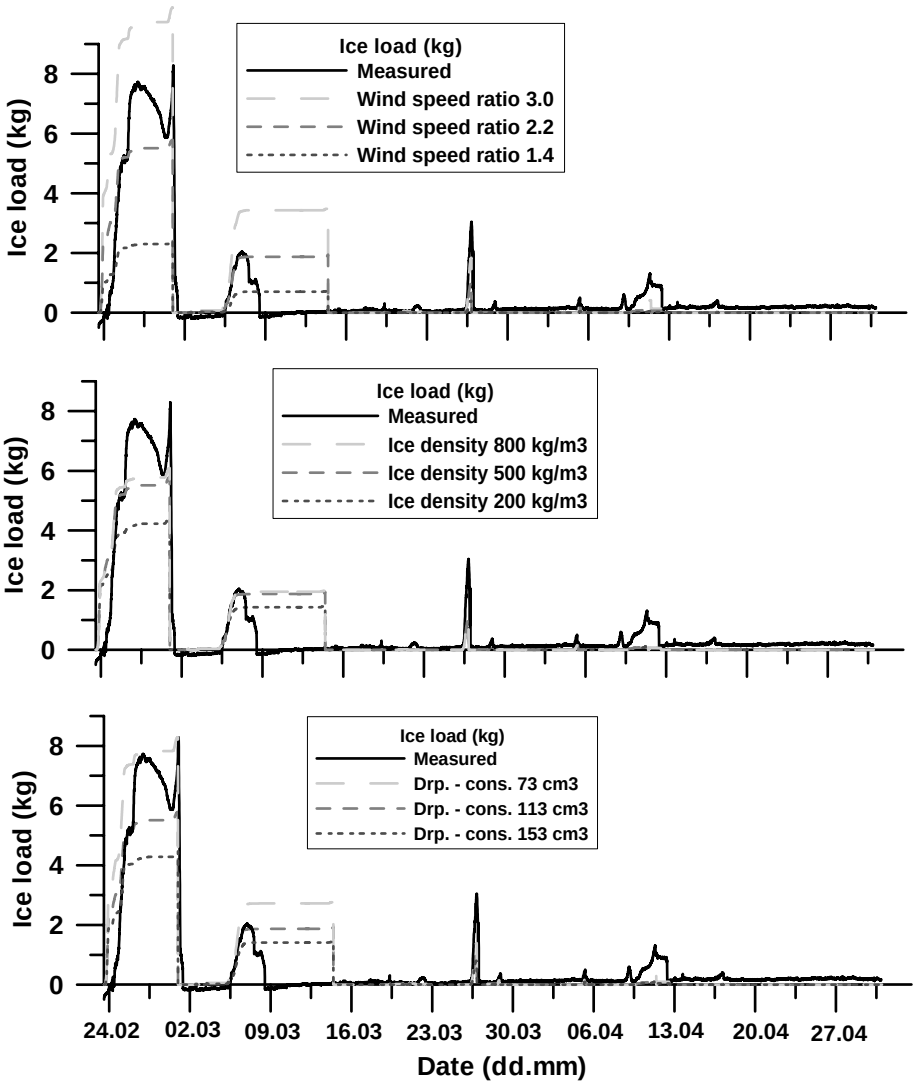

Figure 5.6. Measured and estimated icing with the 3.0 cm rotating rod, from February 23 to May 1, 2004, for varying wind speed ratio (upper), ice density (middle) and droplet concentration (lower).

5.2 Gaustatoppen

At Gaustatoppen data were recorded continously between October 17 and December 16, 2003, and between January 24 and May 5, 2004. The ice scale, with a 3 cm rotating rod, was mounted at the peak and several incidents of icing occured (figure 5.7 and 5.8)..

5.2.1 Modelled ice load between October 17 and December 16, 2003.

Modelled ice load, from the model described in chapter 5.1.4 above and in paper 2, are plotted in figure 5.7. Data, from the station at 1160 m a.s.l., were applied in order to estimate LWC, air temperature and wind speed at 1800 m a.s.l. on Gaustatoppen. It should be noted that the maximum calibrated load of 100 kg (paper1) was reached on November 28, 2003. This makes the accuracy of the measurements from 100 to 150 kg questionable, even if the maximum recordable load is 150 kg.

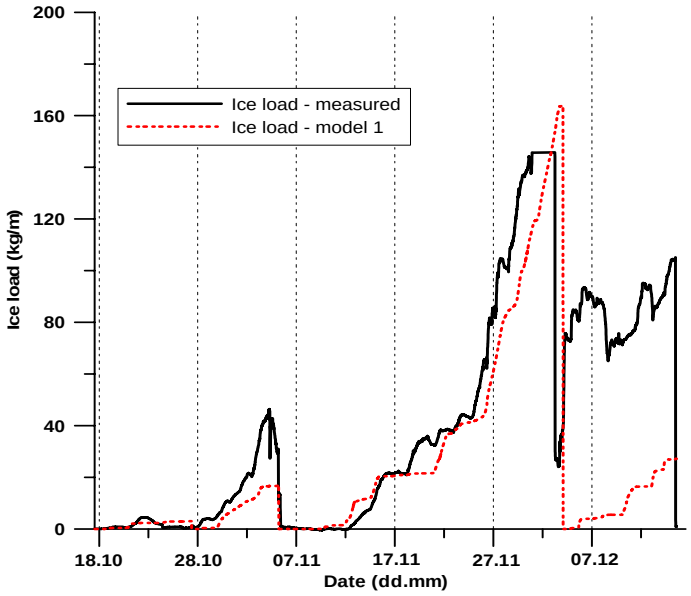

Figure 5.7: Measured and simulated ice load on the 3 cm diameter rotating rod at 1800 m a.s.l at Gaustatoppen during the period October 17 to December 16, 2003.

A. Wind speed
The wind speed on Gaustatoppen, at 1800 m a.s.l., is, on average, higher than at 1160 m a.s.l. by a factor of 1.9, with a standard deviation of 0.6. These values were obtained from one year of wind speed data. Incidents with air temperature ≤0ºC, and relative humidity was ≥96%, were excluded due to the possible effect of icing onto the sensors. During the period October 17 to December 16, 2003, the wind speed sensor stopped several times. This was identified as icing onto the sensors, and a linear interpolation between missing data was therefore carried out.

B. LWC
LWC was estimated by the method described in paper 2. Occasionally, the relative humidity at the lower, (1160 m a.s.l.) station was 100%. An underestimate of LWC was then expected in such conditions.

Figure 5.7 shows that the model detect all the icing incidents as well as the trend in the ice growth with good accuracy. The model drop in ice load November 04 correspond well with a sudden decrease in measured ice load. However, the ice load measurements indicates that not all ice is falling off.

5.2.2 Modelled ice load between January 24 and May 05, 2004.

Results of ice load by the model described in chapter 2 above and in paper 2, is plotted in figure 5.8. Data from the weather station at Møsstrand, 977 m a.s.l., was applied in order to estimate LWC and air temperature. Wind speeds on Gaustatoppen, at 1800 m a.s.l were estimated using ECMWF-model data (European Centre of Medium Range Weather Forecast), with analysis data was given every 6 hours.

A. Wind speed
Wind speed was measured by the sonic wind speed sensor (Gill-instrument, paper 1), from May 30 up until June 26, 2002, at 1800 m a.s.l. at Gaustatoppen. A comparison of the modelled (HIRLAM10) wind speed at the 850-hPa level and the measured wind speed at 1800 m a.s.l. showed that the wind speed at 1800 m a.s.l. was on average, higher than that at 850 hPa by a factor of 1.24, with a standard deviation of 0.55. Measured and recalculated simulated wind speed of this period is plotted in figure 5.9.

B. LWC

The method for estimating LWC was based upon the assumption of an adiabatic increase in LWC with height. The difference between estimated and actual LWC increases with increasing stability. Applying the method for estimating LWC for situations of high stability result in the LWC being overestimated, given the theory outlined in paper 2.

Modeled ice load during this period shows a high overestimation (figure 5.8). This is partly due to the fact that no sublimation is considered. The trend in the ice growth is fairly good reproduced. The ice is modeled to fall of when the air temperature at 1800 is eqaul or higher than 0˚C. The high difference in elevation from 977 m a.s.l. at Møsstrand to 1800 m a.s.l. at Gaustatoppen makes the model sensitiv when the actual air temperature at the top is close to 0˚C. This results sometimes in modeled ice falling off like April 06, while the measured shows no such drop in ice load.

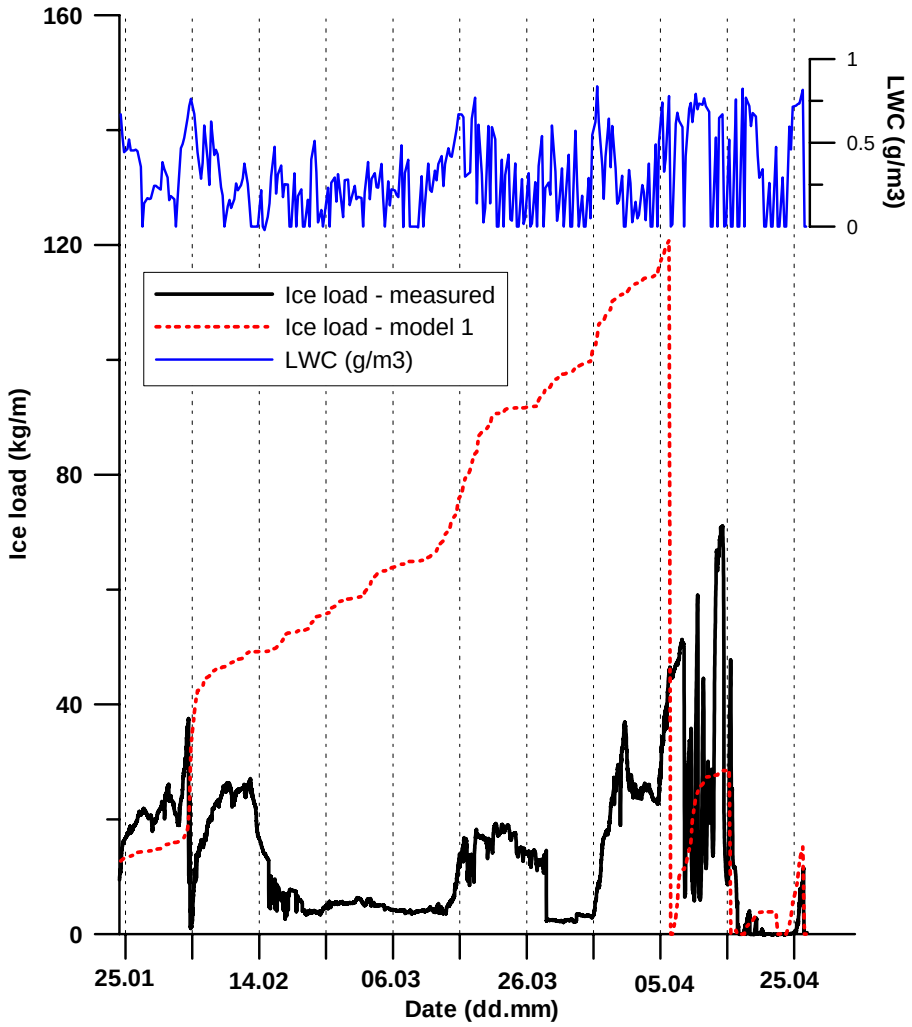

Figure 5.8: Estimated LWC (g/m^3) and measured and simulated ice load on the 3 cm diameter rotating rod at 1800 m a.s.l at Gaustatoppen during the period January 24 to May 5, 2004.

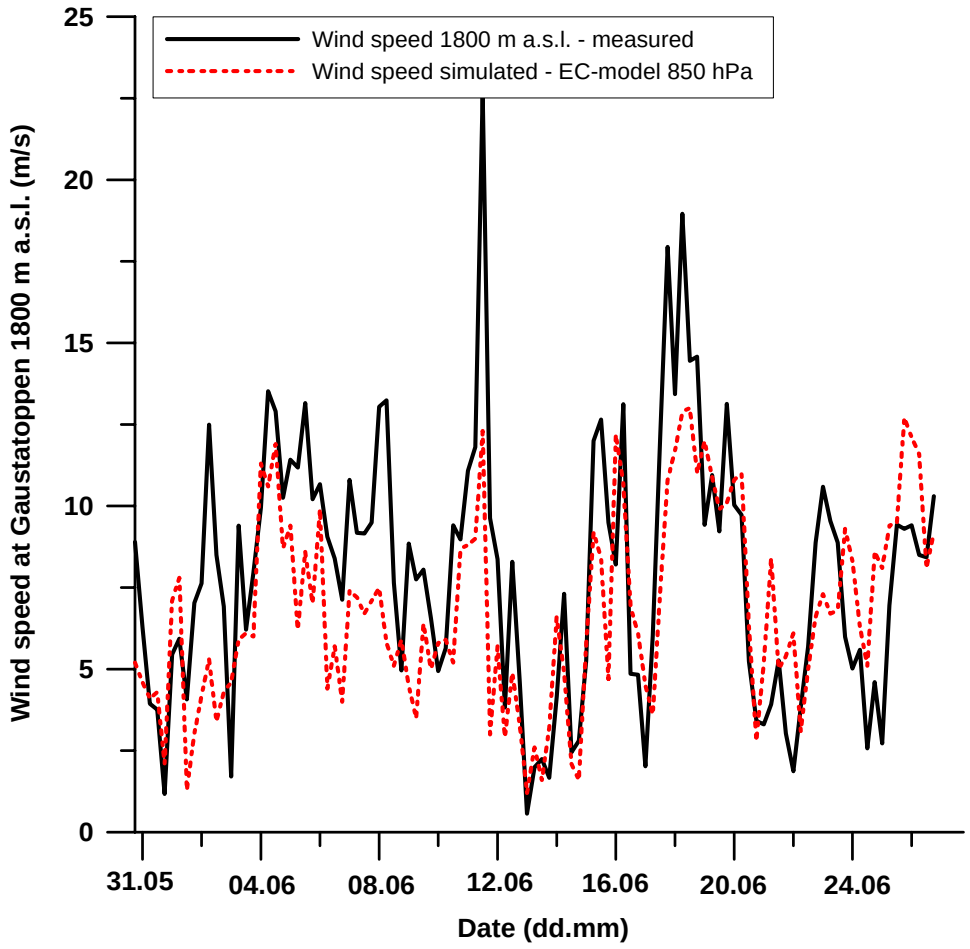

Figure 5.9. Wind speed (m/s) measured by Gill-sonic anemometer and simulated by HIRLAM10-850hPa during the period May 31, to June 27 2002.

LWC on the mountain top (1800 m a.s.l), estimated from measurements from Gaustatoppen at 1160 m a.s.l. and from Møsstrand at 977 m a.s.l. between April 02 and May 05 is plotted in figure 5.10. Estimated wind speed is also included in the figure. LWC estimated from weather data at Møsstrand was, in most cases, higher than LWC estimated from the station at 1160 m at Gaustatoppen. This can be explained by the effects mentioned above, such as high stability or that the station at 1160 m was above the cloud base. Noteworthy is the estimated LWC from the Møsstrand-data from April 30 to May 2, 2004. No LWC was estimated from the station on Gaustatoppen at 1160m. At the same time, a low wind speed was simulated from EC-850 hPa-

data. Nevertheless, the comparison shows a good correlation between estimated LWC by the two different methods.

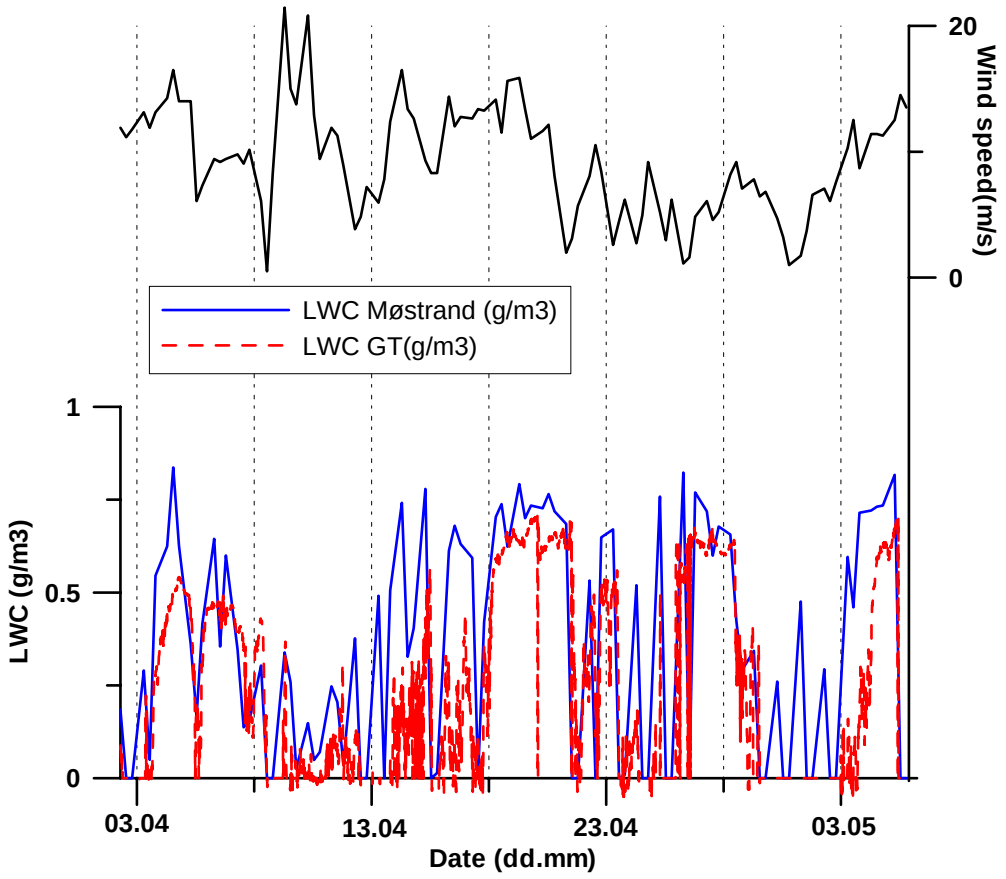

Figure 5.10. Estimated LWC (g/m^3) by the weather station at Møsstrand 977 m a.s.l. (blue curve) and Gaustatoppen 1160 m a.s.l. (red curve), plotted wind speed (m/s) simulated by EC-model.

5.3 Ice detection criteria

A simple test to identify icing conditions on Gaustatoppen between October 18 and December 16, 2003, and on Brosviksåta between February 01 and February 23, 2004, is presented in figure 5.11, 5.12 and 5.13. The requirements for icing conditions is only estimated positive LWC and air temperature <0ºC. The ice detector returns value 0 if one of the requirements is not fulfilled, and a value 1 if both is fulfilled. The plots show a good correlation between icing conditions

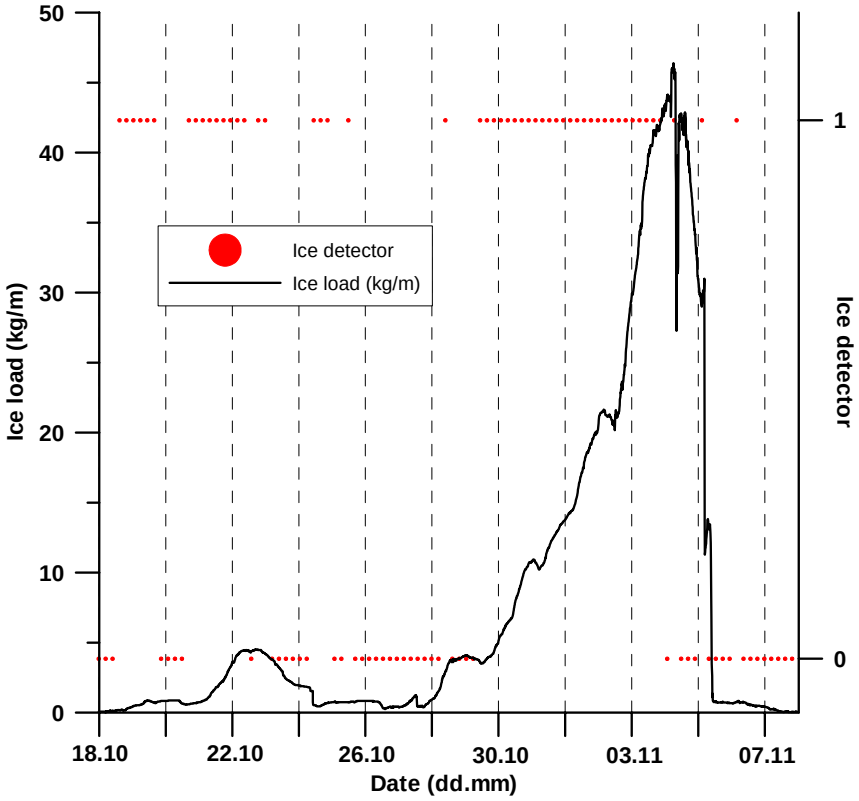

Figure 5.11 Measured ice load and detected icing conditions measured by the ice scale and identified by the ice detector between October 18 and November 08, 2003 at 1800 m a.s.l. at Gaustatoppen.

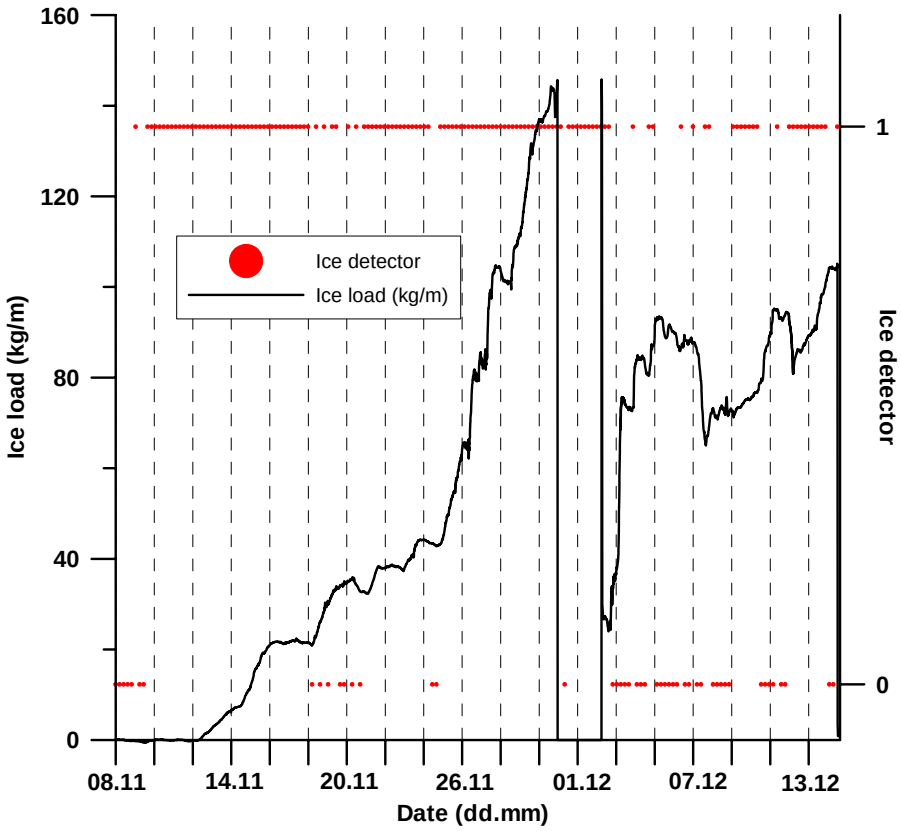

Figure 5.12 Measured ice load and detected icing conditions measured by the ice scale and identified by the ice detector between November 08 and December 16, 2003 at 1800 m a.s.l. at Gaustatoppen.

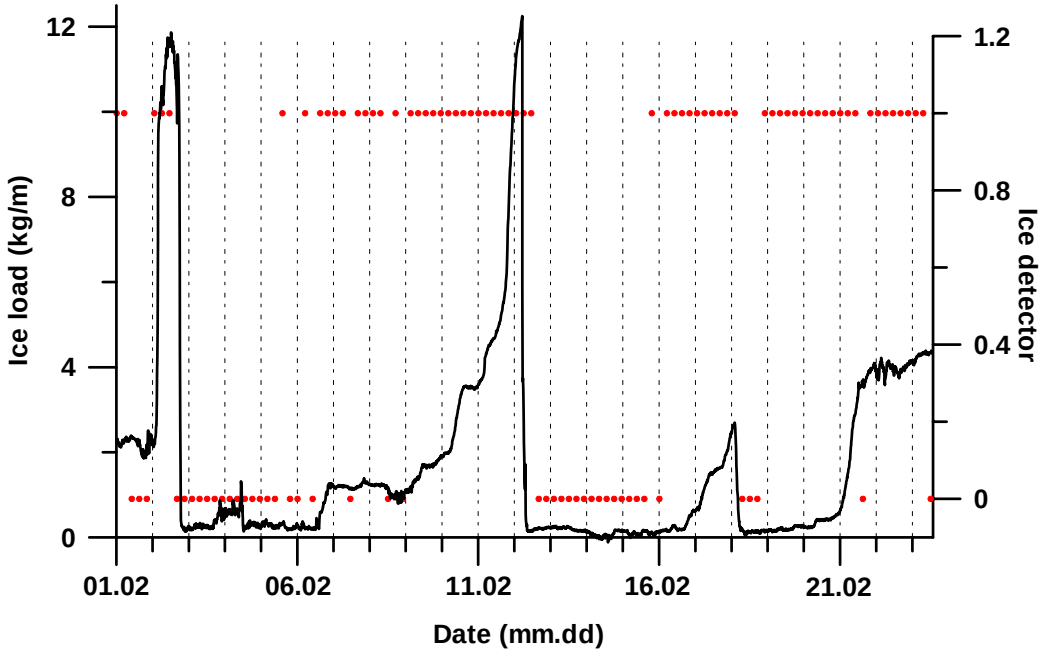

Figure 5.13 Measured ice load and detected icing conditions measured by the ice scale and identified by the ice detectoion between February 01 and February 23, 2004 at 723 m a.s.l. at Brosviksåta.

.

6. Summary and conclusion

The previous chapters reveal that the research in the area of atmospheric icing by in-cloud icing has aspects that have to be further investigated in the future. The theoretical models of ice growth on a cylindrical object are well documented as isolated phenomena, such as in a controlled laboratory. However, the limitation of these methods is the need of detailed information, such as the median volume droplet size, and thereby the cloud droplet size spectrum. The cloud droplet concentration is another parameter that is highly uncertain. Further investigation is therefore needed.

A total of three prototype ice scales for measuring atmospheric icing have been built, tested and calibrated. They have been run for, all together, 34 months at different locations, both in mountainous regions in southern Norway and a coastal area in the north of the country. The ice scale systems have proved to provide useful and reliable data for testing and verification of icing models. For vertical force, tests of the ice scale indicated that ice weight can be measured with an absolute accuracy of approximately 0.125 kg. The standard deviation, as calculated in the laboratory, was 0.027 kg.

The density (ρ_{LWC}) of cloud liquid water content (LWC) is an important parameter for estimating icing on structures as in-cloud icing. A method for calculation of ρ_{LWC} has been described. The method only requires measurements of air temperature, air humidity and wind speed at a known level at unsaturated conditions. These parameters were measured at different levels along the slope of the mountains Brosviksåta (723 m a.s.l.) and Gaustatoppen (1882 m a.s.l.). The beginning and end of the icing period was determined to a high degree of accuracy with this method. Reliable prognoses of ρ_{LWC} will greatly improve the procedures of forecasting duration and intensity of in-cloud icing.

A mesoscale model (MM5 identified the start and end times of the icing event with a high degree of accuracy. On the other hand, the accuracy of the simulated icing intensity was not that good. It is not taken for granted that a high resolution forecast would be more accurate than a forecast using a coarser resolution. Further studies of real-time cases on real-time systems at coarser model resolutions will therefore reveal the capability of MM5 for making reliable daily forecasts of freezing events.

Measurements of accumulated ice on a set of sticks around the ridge of a mountain peak show that even small variations in the location can cause large variations in accreted ice. Existing methods for estimating design load for construction in such harsh environments are based upon the actual height of the site above sea level, together with climatologically data from synoptic weather stations or airports. To improve the estimates of in-cloud icing in the vicinity of the mountain peak several efforts may be undertaken. In this case, the application of micro scale numerical models, like computational fluid dynamics, to describe the wind field around the mountain peak, or measurements at the location for a short period of time, gave valuable information. A basic understanding of the air flow around isolated mountain peaks is vital to understand how complex topography and changing wind direction strongly influence icing intensity.

Observations during the 1998 winter show an excessive sea spray ice build up on the old Melkøya breakwater, which indicates that icing problems can be far more severe than normally expected on near shore installations in Northern Norway. The study focused on describing the weather situation leading to the documented ice build up. Based on this, preparing predictions as to the frequency and severity of the icing can be done.

Melkøya is very exposed to wind which reduces potential snow and snow drift problems at the Liquid Natural Gas (LNG) plant. Wind conditions has been modelled and measured. Results were used as input for the estimates of icing and snow conditions. In addtion, they were used as a basis for a general review of the defined wind profile for wind load predictions.

7. REFERENCES

Aasen, S. E., 1995. The Skipheia Wind Measurement Station – Instrumentation, Wind speed profiles and Turbulence spectra, Dr. Scient thesis, University of Trondheim, ISBN-82-90896-89-1.

Ahti, K. and Makkonen, L., 1982. Observation on rime formation in relation to routinely measured meteorological parameters, Geophysica, 19(1): 75 – 85.

Finstad, K. J. and Lozowski, E. P. and Gates E. M.,1988a. A computational investigation of water droplet trajectories, J. Atmos. and Oce, Tech., 5: 160 – 170.

Finstad, K. J., Lozowski, E. P. and Makkonen L., 1988b. On the median volume diameter approximation for droplet collision efficiency. J. Atmos. Sci. 45: 4008 - 4012.

Gjessing, Y. T., Skartveit, A. and Utaaker, K., 1990. Vurdering av sikt- og vindforhold på Hurumåsen. Meteorological Report Series University of Bergen. 1: 1 – 49.

Haldar, A. P., McComber, P., Marshall, M. A., Ichac, M., Goel, A. and Katselein, M., 1996. Validation of ice accretion models for freezing precipitation using filed data, Proceeding 7th International Workshop on Atmospheric Icing of Structures, pp. 189 – 194.

Harstveit, K., 2002. Using routine meteorological data from airfields to produce a map of ice risk zones in Norway. Proceeding 10th International Workshop on Atmospheric Icing of Structures, CD: Session 8-1.

ISO 12494, 2001. ISO (the International Organization for Standardization) 12494 – Atmospheric icing of structures.

Langmuir, I. and Blodgett, K. B., 1946. A mathematical investigation of water droplet trajectories. Collected Works of Irwing Langmuir, Pergamon Press, 10: 348 – 393.

Ludlam, F. N., 1951. The heat economy of rimed cylinder. Quart. J. Roy. Meteor. Soc., 77: 663 – 666.

Makkonen, L., 1984a. Modeling of ice accretion on wires, J. Climate Appl. Meteor., 23: 929 – 939.

Makkonen, L. and Stallabras, J. R., 1987. Experiments on the cloud droplet collision efficiency of cylinders, J. of Clim. Appl. Meteor., 26: 1406 – 1411.

Makkonen, L. and Ahti, K. 1995. Climatic mapping of ice loads based on airport weather observations, Atmos. Res., 36: 185 – 193.

Makkonen, L., 1996. Modeling power line icing in freezing precipitation, Proceeding 7th International Workshop on Atmospheric Icing of Structures, pp. 195 – 200.

Mazin, I. P., Korolev, A. V., Heymsfield, A., Isaac, G. A. and Cober, S. G., 2001. Thermodynamics of icing cylinder for measurements of liquid water content in supercooled clouds, J. Atmos. and Oce, Tech., 18: 543 – 558.

Mulherin, N. D., 1988. Atmospheric icing and communication tower failure in the United States. Cols regions Science and Technology, 27: 543 – 558.

Nicholls, S., 1984. The dynamics of stratocumulus: aircraft observations and comparisons with a mixed layer model, Q. J. R. Meteor. Soc., 110: 783 – 820.

Noonkester, V. R., 1984. Droplet spectra observed in marine stratus cloud layers, J. Atmos. Sci., 41: 829 – 845.

Poots, G., 2000. Ice and snow accretion on structures. Phil. Trans. R. Soc. Lond. A (200), 358: 2799 – 3033.

Schemenauer, R. S., Macpherson, J. I., Isaac, G. A. and Strapp, J. W., 1980. Canadian participation in HIPLEX 1979. Report APRB 110 P 34, Atmospheric Environment Service, Environment Canada, 206 pp.

Sundin E. Makkonen L., 1998. Ice loads on a lattice tower estimated by weather station data. J. Appl. Meteoror. 37: 523-529.